

Sphercity study for e^+e^- Fragmentation Functions using Pythia MC generator

H. Bello Martínez*, R. J. Hernández-Pinto, I. León Monzón

Facultad de Ciencias Físico-Matemáticas, Universidad Autónoma de Sinaloa, Ciudad Universitaria, CP 80000, Culiacán, Sinaloa, México.

E-mail: hectorbm884@gmail.com, roger@uas.edu.mx, ildefonso.leon.monzon@cern.ch

The Fragmentation Functions is one of the non-perturbative components of the QCD factorization theorem. They represents the probability of a parton carrying a fraction z of momentum to form into a particular kind of hadron. In this work, we study the jet fragmentation functions in the collisions between electrons and positrons. The jets were identified with Fastjet for different p_T^{chjet} intervals. The intervals and the final jets were reconstructed by means of the event shape separation using sphercity variable, the study is performed under Pythia Monte Carlo event generator framework.

*7th Annual Conference on Large Hadron Collider Physics - LHCP2019
20-25 May, 2019
Puebla, Mexico*

*Speaker.

1. Introduction

¹ In recent years the Large Hadron Collider (LHC) has obtained very interesting results in the study of systems created in pp collisions at center of mass energy of the order of TeV. In addition, past results at CERN for e^+e^- have motivated to start new studies in new accelerator facilities such as the Future Circular Collider (FCC) at greater energies [2, 3, 4, 5]. Furthermore, there is an increasing interest to make studies in these two colliding systems, due to the fact that the FCC will collide not only protons but electrons and positrons. The study of the final states particles produced after the collision gives useful information of the hadronization process [6]. In particular, the study of fragmentation functions (FF) helps to understand and should model the theory behind this non-perturbative phenomena [7, 8]. On the other hand, sphericity analysis [11] is a tool that has taken a great interest for studying the event shapes of final states charged particles [12] and hadrons [13, 14]. Important results had been obtained by computing the production of reconstructed jets with Fastjet [19] after the hadronization process [15, 16, 17, 18]. There have been recent studies in which they consider to join these topics together at generator level using Pythia [21, 22, 23], in order to extract a more differential analysis of the final states created in e^+e^- collisions.

In this work, we study the fragmentation functions for jet production using two different approaches for jet reconstruction, the anti- k_T algorithm and the sphericity analysis, this was done using Pythia 6 and 8 Monte Carlo event generators.

1.1 Fragmentation Functions

The final stage hadron, $d\sigma/dz$, in general is described by mean of the QCD factorization theorem [6]. It allows us to compute observables in terms of short range quantities (calculable in perturbative QCD) and long range quantities (not calculable in perturbative QCD), which are momentum fraction z dependent. The fragmentation functions are defined as follows:

- For electron positron annihilation, due to the lack of internal structure of electrons in the process $e^+e^- \rightarrow \gamma/Z^0 \rightarrow h + X$, the hadro-production cross section leads to the description of the fragmentation function $F^h(z, s)$ as [8]:

$$\frac{1}{\sigma_0} \frac{d\sigma^h}{dz} = F^h(z, s) = \sum_i \int_z^1 \frac{dz}{z} C_i(z, \alpha_s, \frac{s}{\mu^2}) D_i^h(z, \mu^2) + \mathcal{O}(1/\sqrt{s}), \quad (1.1)$$

here σ_0 is a normalization factor, i runs for all quarks and gluons, $D_i^h(z, \mu^2)$ are the fragmentation densities that describes the probability that the parton i fragments into a hadron h . the C_i are the observable-dependent coefficient functions whose NLO and NNLO terms are known [9, 10], and $z = \frac{2p_h \cdot q}{q^2}$. In practice the approximations $z \approx 2P_h/\sqrt{s}$ and $z \approx 2E_h/\sqrt{s}$ are used.

- For jets, the jet production cross section is given by

¹This contribution is based on our work [1]

$$\frac{d\sigma^{chjet}}{dp_T d\eta}(p_T^{chjet}) = \frac{1}{\mathcal{L}_{int}} \frac{\Delta N_{jets}}{\Delta p_T \Delta \eta}(p_T^{chjet}), \quad (1.2)$$

where it has been defined the scaling variable $z^{ch} = p_T^{particle} / p_T^{chjet}$, and the jet fragmentation function is defined [18] as:

$$F^z(z^{ch}, p_T^{chjet}) = \frac{1}{N_{jets}} \frac{dN_{jets}}{dz^{ch}}. \quad (1.3)$$

It is worth mentioning that a precise knowledge on FFs is vital for the quantitative description of a wide variety of hard scattering processes and the understanding of phenomena produced by jets [12, 16, 17, 18].

1.2 Jet reconstruction methods, anti- k_T algorithm and sphericity

One of the implemented algorithm in Fastjet [19] for jet reconstruction is the anti- k_T [20]. It consists in taking the beam jet axis B , and to select all the particles i with distance $d_{iB} = 1/p_{Ti}^2$, inside the radius $\Delta R_{ij}^2 = (y_i - y_j)^2 + (\phi_i - \phi_j)^2$. The distance among each particles pair i, j is given by,

$$d_{ij} = \min(1/p_{Ti}^2, 1/p_{Tj}^2) \Delta R_{ij}^2 / R^2. \quad (1.4)$$

On the other hand, the event shape called transverse sphericity [11] is defined as,

$$S_T^{sphericity} = S_O = \frac{\pi^2}{4} \min_{\vec{n}=(n_x, n_y, 0)} \left(\frac{\sum_i |\vec{p}_{Ti} \times \vec{n}|}{\sum_i |\vec{p}_{Ti}|} \right)^2, \quad (1.5)$$

where the values which defines the structure in the transverse plane runs from 0 (for jetty) to 1 (for isotropic). It is remarkable that the two methods are essentially different and their use should provide complementary information. This naive conclusion is based on the fact that in Fastjet we have an η dependence due to the selection of radius of the cone but in sphericity there is only ϕ dependence. Furthermore, with sphericity only back to back dijet shapes can be selected, meanwhile in Fastjet this feature is not limited, see Figure 1.

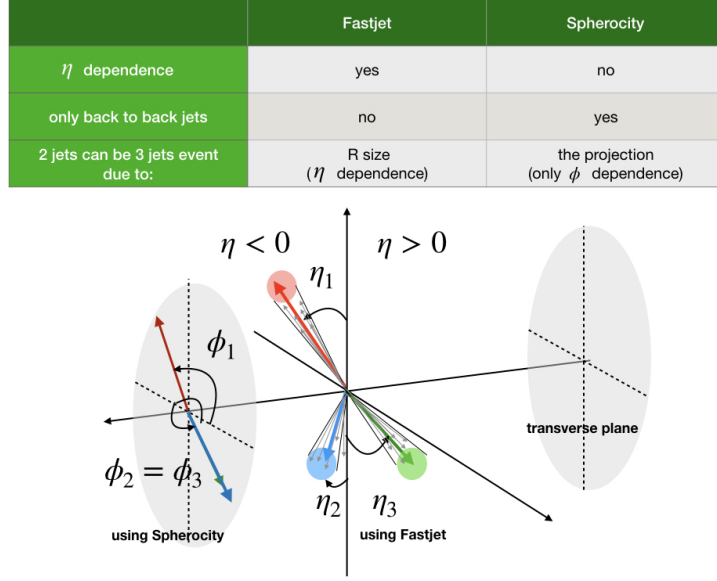


Figure 1: Graphical description of the two different methods for jet reconstruction explaining the complementarity of the methods.

1.3 Fragmentation Functions in Pythia

The FF inside Pythia 6.4 [21] and Pythia 8.2 [22] is basically given by the Lund symmetric FF as [24]:

$$f(z) \propto z^{-1} (1-z)^a \exp\left(\frac{-bm_{\perp}^2}{z}\right), \quad (1.6)$$

where m_{\perp}^2 is the hadron transverse mass squared, z is the fraction hadron to parton momentum and the free parameters a and b are related to the total multiplicity; these parameters govern the shape of the FF, and must be constrained by fits to data. Roughly speaking, large value for a suppress the hard region $z \rightarrow 1$, while a large value for b suppresses the soft region, $z \rightarrow 0$. For Pythia 6.4 [21] these values are set to $a = 0.3$, $b = 0.58$; and Pythia 8.2 is using the Monash tune [18], where the default values are, $a = 0.68$, and $b = 0.98$.

2. Event selection

For the simulation, we generate 30 million of events in Pythia 6.4 [21] and Pythia 8.2 [22] using tune Monash [23] for e^+e^- collisions at $\sqrt{s} = 91$ GeV, using DELPHI kinematic cuts [25], at least 5 stable charged particles within $0.3 < p < 70$ GeV, $E > 15$ GeV and $0.01 < z < 1$.

For jet reconstruction, the anti- k_T algorithm was used with the kinematical cuts $p_{T,min} = 5$ GeV, $\eta_{jet} < 0.5$ and $R = 0.4$, and finally we use the p_T recombination scheme as in ALICE method [18]. For the sphericity study, the percentile selection (S_{Opc}) was taken in intervals of 10% as it was done in Ref. [12].

3. Results

First we present the FF for pions and kaons produced in e^+e^- collisions at $\sqrt{s} = 91$ GeV, in Figure 2 and Figure 3, we compare our results with available data from DELPHI [25], SLD [26] and ALEPH [27]. For the pions case (Figure 2) the difference is within 5% (in Pythia 6.4) to 20% (in Pythia 8.2). For the kaons case (Figure 3) the difference goes from 20% (in Pythia 6.4) to 40% (in Pythia 8.2), which is expected due to the poor determination of strangeness production in Pythia. It is important to notice that the best agreement is given for the comparison with DELPHI also with the wide binning range of the available data.

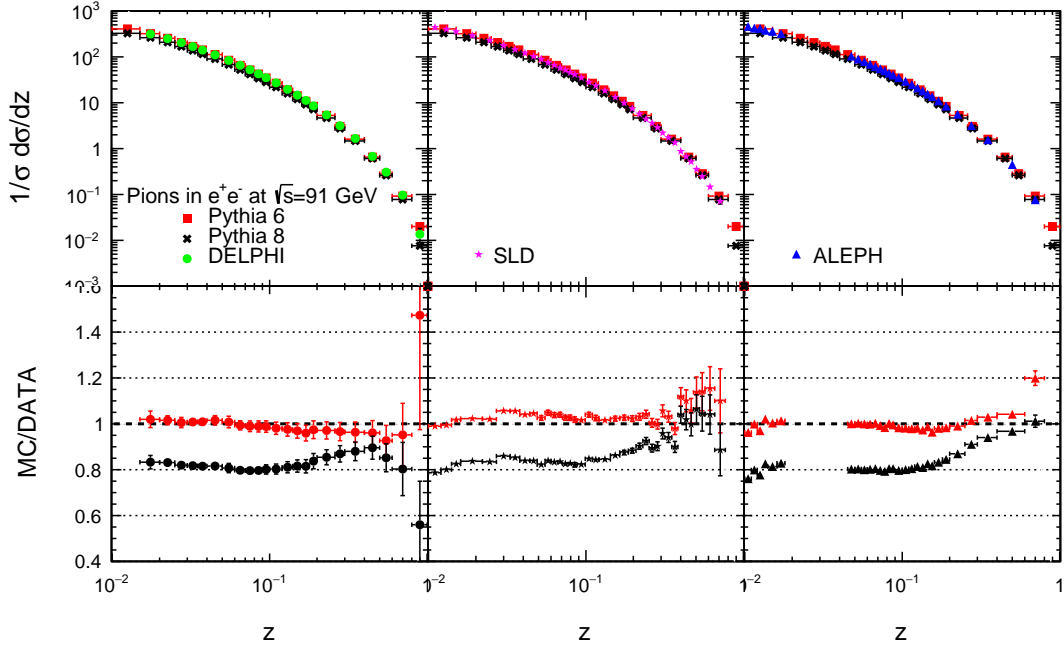


Figure 2: On top, the pions FFs (top) for e^+e^- at $\sqrt{s} = 91$ GeV. Pythia 6.4, Pythia 8.2, DELPHI [25], SLD [26] and ALEPH [27] data are shown. On bottom, the comparison data to Monte Carlo.

Based on these results, we proceed with the analysis for jets reconstructed with FastJet and the event shape characterization with sphericity.

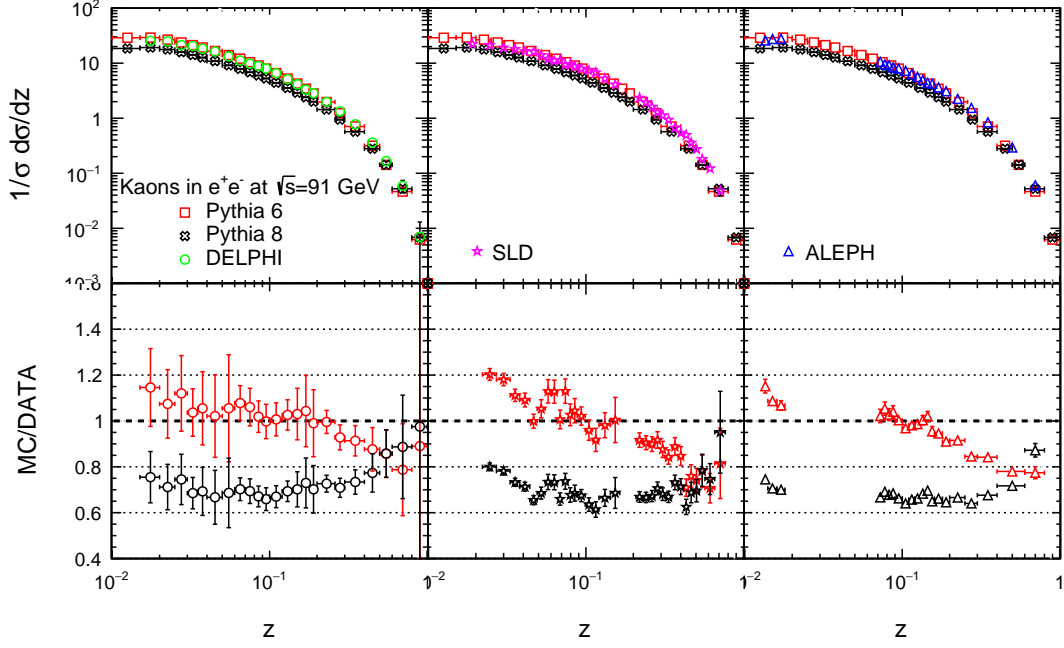


Figure 3: On top, the kaons FFs (top) for e^+e^- at $\sqrt{s} = 91$ GeV. Pythia 6.4, Pythia 8.2, DELPHI [25], SLD [26] and ALEPH [27] data are shown. On bottom, the comparison data to Monte Carlo.

3.1 Jets with Fastjet

We present in Figure 4 the results for jets reconstructed in different jet transverse momentum intervals. As expected, we obtain large probabilities in the regime of high z and low p_T^{chjet} , this behaviour is opposite in the small z region. Furthermore, a crossing point was found around $z = 0.3$. A comparison with the inclusive sample (no p_T^{chjet} separation) shows clearly the behaviour.

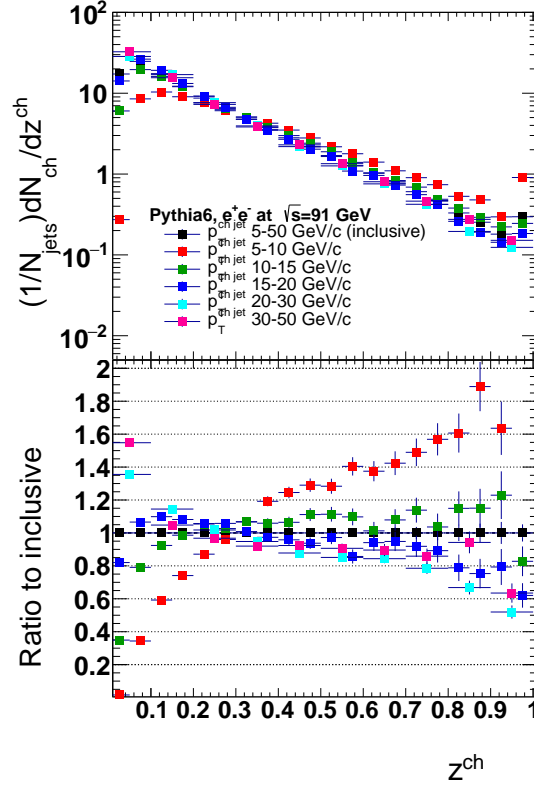


Figure 4: On top, charged jet fragmentation function, results for e^+e^- collisions are shown for $p_T^{ch,jet}$ selection, from the lower (red) to higher (magenta) intervals. On bottom, ratio to inclusive is shown.

3.2 Sphericity separation

In this section, we present the results for e^+e^- collisions, for sphericity separation in different sphericity percentile intervals. We observe in Figure 5 (left) that for jetty events ($0 < S_{Opc} < 10\%$) the greater probability for fragmentation is given as z increases. The comparison of the remaining sphericity percentile intervals with respect to the jetty events shows a variation of the fragmentation as the event shape gets isotropic. A crossing point was found as at $z = 0.15$ as shown in Figure 5 (right). Also, we found that at high z values the difference increases.

4. Conclusions

We have presented an analysis using the anti- k_T jet reconstruction algorithm and also a new method to study the fragmentation functions for jets, based on the event shape called sphericity. From the Fastjet analysis we obtain that for high $p_T^{ch,jet}$ the probability for hadron formation decrease at high z compared to low $p_T^{ch,jet}$. From the sphericity analysis we observe that the greater probability for fragmentation at large z is given for jetty events.

This analysis could be used as a proposal to study these effects in real data at LHC and in the future FCC and also for tuning high energy Monte Carlo generators.

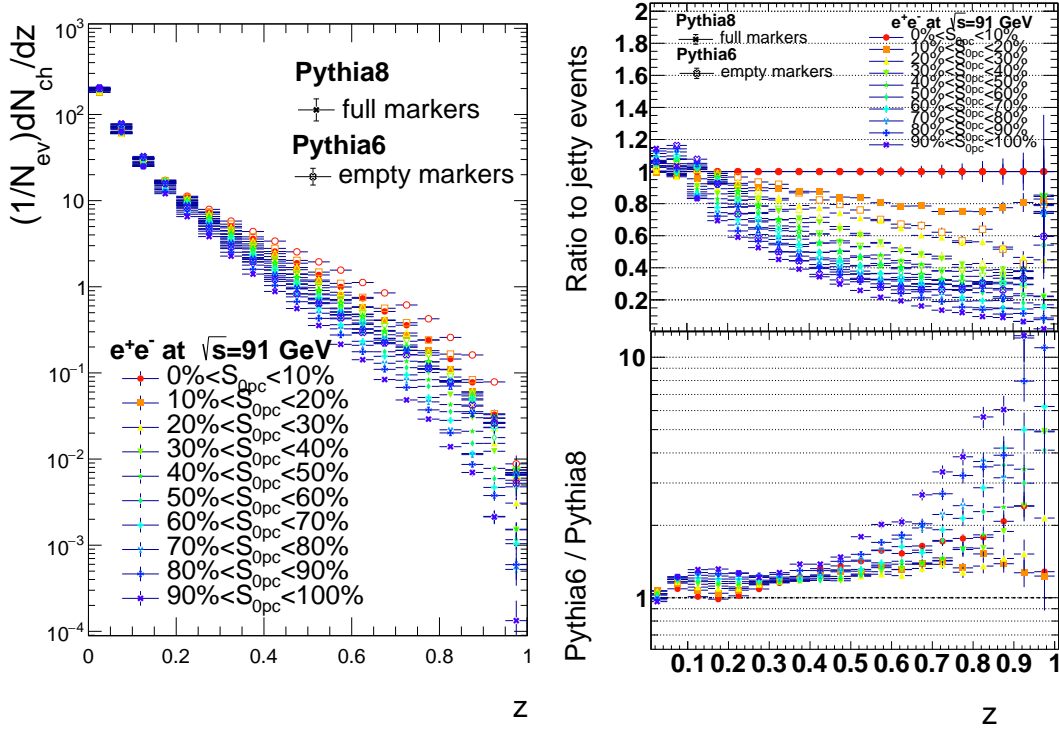


Figure 5: Left-hand side: Sphericity separation for fragmentation functions, results for e^+e^- collisions, the 10% of the most jetty (red points) and isotropic (blue points) events are shown. Right-hand side: It's shown the ratio of each sphericity percentile intervals to jetty events ($0 < S_{0pc} < 10\%$) (on top), and the ratio of Pythia 6.4 to Pythia 8.2 results (on bottom).

5. Acknowledgements

The authors want to thank the support for this provided from CONACYT and the COST Action CA16201 PARTICLEFACE. H.B. want also to thank to CONACYT for the postdoctoral fellowship and also thank to the Parque de Innovacion Tecnologica (PIT-UAS) for the computational facilities at UAS.

References

- [1] H. Bello Martinez, J. R. Hernández Pinto and I. León Monzón, in preparation.
- [2] A. Abada et al. (FCC Collaboration), *Eur. Phys. J. C* (2019) 79: 474.
- [3] A. Abada et al. (FCC Collaboration), *Eur. Phys. J. Spec. Top.* (2019) 228: 261.
- [4] A. Abada et al. (FCC Collaboration), *Eur. Phys. J. Spec. Top.* (2019) 228: 755.
- [5] A. Abada et al. (FCC Collaboration), *CERN-ACC-2019-0006*
- [6] S. Albino, *Rev. Mod. Phys.* 82, 2489 (2010),
- [7] D. de Florian, R. Sassot, M. Epele, R. J. Hernandez-Pinto, and M. Stratmann, *Phys. Rev. D* 91, 014035 (2015).

- [8] M. Tanabashi et al.(PDG), *Phys. Rev. D* **98**, 030001 (2018)
- [9] Baier, R., and K. Fey, *Z. Phys. C* **2**, 339.1979
- [10] Mitov, A., and S. Moch, *Nucl. Phys. B* **751**, 18. 2006,
- [11] A. Banfi, G. P. Salam, and G. Zanderighi, *JHEP* **0408** (2004) 062.
- [12] ALICE collaboration, [arXiv:1905.07208](#) CERN-EP-2019-094, submitted to EPJC.
- [13] Gyula Bencedi for ALICE Collaboration, *Nuclear Physics A* **00** (2018)
- [14] Vislavicius for ALICE Collaboration, *Nucl. Phys. A*, **967** (2017), p. 337
- [15] H. Bello, A. Fernandez Tállez, A. Ortiz, *J.Phys.Conf.Ser.* **761** (2016) no.1, 012033
[arXiv:1609.00692 \[hep-ex\]](#)
- [16] A. Ortiz, G. Bencedi, H. Bello, *J. Phys. G: Nucl. Part. Phys.* **44** (2017) 065001 [arXiv:1608.04784 \[hep-ph\]](#)
- [17] ALICE collaboration, *Phys. Rev. D* **91** (2015) 112012.
- [18] ALICE collaboration, *Phys. Rev. D* **99**, 012016 (2019) [arxiv:1809.03232](#)
- [19] M. Cacciari and G.P. Salam, *Phys. Lett. B* **641** (2006) 57.
- [20] M. Cacciari, G. P. Salam and G. Soyez, *JHEP* **0804**(2008) 063 [arXiv:0802.1189 \[hep-ph\]](#)
- [21] T. Sjostrand et al., *JHEP* **0605** (2006) 026 [hep-ph/0603175](#).
- [22] T. Sjostrand et al., *Comput. Phys. Commun.* **191**(2015)159–177. [arXiv:1410.3012](#)
- [23] P. Skands, S. Carrazza, J. Rojo, *Eur. Phys. J. C* **74**(8) (2014) 3024. [arXiv:1404.5630](#),
- [24] B. Andersson, *Camb. Monogr. Part. Phys. Nucl. Phys. Cosm.*, 1997
- [25] DELPHI Collaboration *Eur. Phys. J. C* **5**, 585–620 (1998)
- [26] SLD Collaboration *Phys. Rev. D*, Vol **59**, 052001
- [27] ALEPH Collaboration *Z. Phys. C* **66**, 355-365 (1995)